Magnetic reversal in ion-irradiated FePt thin films

A Mougin, J Ferré, O Plantevin, H Cruguel, F Fortuna, H Bernas, A Marty, C Beigné, Yves Samson

Magnetic reversal in ion-irradiated FePt thin films

A. Mougin and J. Ferré

E-mail: mougin@lps.u-psud.fr
Laboratoire de Physique des Solides, Univ. Paris-Sud, UMR CNRS 8502, 91405 Orsay Cedex, France

O. Plantevin, H. Cruguel, F. Fortuna and H. Bernas

Centre de Spectrométrie Nucléaire et de Spectrométrie de Masse, Université Paris-Sud, UMR CNRS-IN2P3 8609, 91405 Orsay Cedex France

A. Marty, C. Beigné and Y. Samson

CEA Grenoble, INAC/SP2M, 38054 Grenoble, France

Abstract. Previous work on ion irradiation control of FePt thin films magnetic anisotropy is extended to ultrathin films (2-10nm). The effects of 30keV He ion irradiation on the magnetic properties are explored as a function of ion fluence and film thickness. *Depending on their growth conditions, the thinnest films exhibit different magnetic properties. Although this affects their final magnetic behaviour,* we show that after irradiation at 300°C the easy magnetization axis may rotate entirely from in-plane to out-of-plane at very low fluences, e.g. 2×10^{13} He^+/cm^2 on 5 nm thick film. This demonstrates the extreme sensitivity of the magnetic anisotropy to ion-induced local $L1_0$ ordering. Under these conditions, ultrathin films may exhibit perfectly square hysteresis loops with 100% remnant magnetization and low coercivity.

PACS numbers: Valid PACS appear here

Submitted to: *J. Phys. D: Appl. Phys.*

1. Introduction

The use of irradiation with low-mass (He) ions at keV energies *allows an* excellent control over the magnetic properties of magnetic thin films or multilayers[1, 2, 3, 4, 5]. As detailed in reference [2], the low interaction cross-sections and very low (eV-scale) energy transfers lead to an absence of damage cascade effects and to a linear fluence-dependent accumulation of individual, very short-range atomic displacements, inducing easily controlled modifications in the atomic short range order, notably at multilayer interfaces ; *these parameters* also control film (or multilayer) strain relaxation [6]. In samples such as ultrathin Co/Pt multilayers, these structural modifications affect the interface component of the magnetic anisotropy, leading to its control in direction and amplitude. This effect was used to perform magnetic patterning at sub-50 nm resolution without affecting the surface roughness [2, 5, 7]. It was also used to control thin film exchange bias effects [3, 1].

Another application of the low ion mass irradiation was *the* control *of* phase changes in thin film alloy structures [8, 9]. In the case of FePt and FePd equiatomic alloy films, the magnetocrystalline anisotropy (MA) is related to the degree of chemical order in the alloy [10, 11, 12]: the largest anisotropy is obtained for the so-called $L1_0$ (fct) phase with alternate Fe and Pt (or Pd) atomic layers along the (001) direction, whereas the pristine films display a A_1 (fcc) structure with Fe and Pt (Pd) randomly occupying all sites. *In the case where* keV He ion irradiation-induced displacements were combined with sufficient in situ heating, *a significant reduction* of the A_1 - $L1_0$ phase transformation temperature *was observed* (300°C instead of $\simeq$670°C). This is advantageous for applications, but insufficient since the ordering may occur along any one of the three energetically equivalent <100> axes. In order to select a single one of the latter (the perpendicular one), we grew our films by molecular beam epitaxy (MBE) via alternate atomic layer-by-layer deposition at room temperature [8]. This led to pristine films with enough initial directional short-range order (DSRO) to impact on the final structure after irradiation-induced ordering. As evidenced by the structural and magnetic properties and supported by Monte Carlo simulations, the ordering then occurs solely along the quadratic *c* axis perpendicular to the film surface, i.e., along a single variant. *In contrast* to temperature-dependent ordering, the irradiation-induced ordering kinetics are entirely due to the action of successive single vacancies. *These vacancies allow* pairwise exchanges and the driving force for ordering *is* the energy gained by maximizing the number of Fe-Pd (or Pt) bonds. Thus, the number of vacancies (hence the irradiation fluence) required to order the alloy should diminish as the film thickness is reduced. In counterpart, our Monte Carlo simulations, which showed reasonable agreement with the experimental ordering rate, assumed the vacancy lifetime to be limited by capture at surfaces or interfaces. This work was mostly performed on films whose thickness was typically 50 nm, i.e. such that the influence of the first atomic layers could be neglected. However, easier vacancies escape may decrease the efficiency of the irradiation in ultrathin films or nanoparticles.

Would these rather simple conclusions be valid if the irradiation method were applied to ultrathin films (at and below 10 nm)? This raises two questions : (i) Under appropriate ion beam conditions, is the rate of pairwise exchanges high enough to induce ordering at significantly lower fluences in thinner films?, and (ii) As previously shown in detail [13, 14], the growth mechanism and hence the film morphology evolve significantly in the initial stages of film growth - up to about twenty atomic layers, and this drastically affects their magnetic properties and one may ask how this will affect their response to irradiation. The purpose of the present work was to evaluate the interaction of these two very different effects, and to determine whether the ion beam ordering mechanism was still operative down to the thinnest available films. Although the magnetic properties of the thinnest pristine films are significantly affected by growth conditions, we find that $L1_0$ ordering definitely occurred after ion irradiation at very low fluences in the 10 nm (or thinner) films. Direct structural measurements via X-ray diffraction were out of reach in the thickness range of our samples, but Magneto-Optical Kerr Effect (MOKE) sensitivity allowed us to deduce information on ordering and to determine the influence of the irradiation process on magnetic properties such as the hysteresis loop and the domain pattern.

2. Theory for understanding thin films magnetism

In order to clarify the discussion below, we briefly recall the various contributions to thin film magnetic properties. The total energy is the sum of the Zeeman energy E_H in the presence of an external magnetic field H, the demagnetizing energy E_D (which increases as the square of the saturation magnetization M_S but also as the thickness t), the anisotropy energy (proportional to the magnetocrystalline anisotropy constant K_u) and the exchange energy (proportional to the exchange constant A). A dimensionless indicator describing the anisotropy strength of thin films is the quality factor Q given by equation (1), which is the ratio between the anisotropy and the magnetostatic demagnetizing energy:

$$Q = \frac{K_u}{2\pi M_S^2} \tag{1}$$

As long as Q is smaller than 1, the demagnetizing energy being larger than the anisotropy energy, the magnetization lies in the sample plane. When Q is larger than 1, the layer magnetization is out-of-plane. The value of Q is a relevant parameter to signal equilibrium domain configurations and hysteresis loops in out-of-plane magnetized samples. In such systems, the long range demagnetizing field tends to impose small domains of opposite magnetization [15]. *Domain formation reduces the demagnetizing energy. On the other hand, the wall energy (directly obtained from the exchange and anisotropy energies) has to be taken into account. Finally, the energy minimum is obtained for a periodic domain pattern.* Consequently, polar hysteresis loops *of such systems are* elongated with some opening at high field, signaling that a large

perpendicular magnetic anisotropy coexists with a low remnant magnetization. In cobalt epitaxial thin films, a complete analysis as a function of thickness was published in [16].

Consider a stripe domain structure in a film where the easy axis is perpendicular to the surface, as described by Kooy and Enz [17]. They assumed that the domain structure was composed of straight domains where the magnetization is parallel (width $d_\uparrow$) or antiparallel (width $d_\downarrow$) to the external magnetic field H applied perpendicular to the sample plane. The demagnetizing field and the (180° Bloch -type) domain walls were also assumed to be perpendicular to the surface. Forming domain walls costs an energy E_W, given by equation (2). It enters the wall-surface energy σ_W that directly reflects the competition between anisotropy and exchange.

$$E_W = \sigma_W \times \frac{2t}{(d_\uparrow + d_\downarrow)} \text{with } \sigma_W = 4\sqrt{AK_u} \tag{2}$$

The Zeeman energy is simply given by Equation 3 as a function of the remnant magnetization M.

$$E_H = -tHM \text{ with } M = M_S \frac{(d_\uparrow - d_\downarrow)}{(d_\uparrow + d_\downarrow)} \tag{3}$$

The demagnetizing energy of the stripes configuration can be written (Equation (4)) in terms of the remnant magnetization and of a geometrical perpendicular demagnetizing factor $N_\perp(M)$.

$$E_D = 2\pi t N_\perp M_S^2 \tag{4}$$

The demagnetizing factor $N_\perp$, taking into account the magnetic charges of the opposite surfaces [17] is mainly determined by the ratio $(M/M_S)^2$ (Equation (5)). It is corrected by an converging serie of terms weighted by the ratio $t/(d_\uparrow + d_\downarrow)$ between the film thickness and the domain size.

$$\begin{aligned} N_\perp = & \left(\frac{M}{M_S}\right)^2 + \frac{8}{\pi^3}\frac{d_\uparrow + d_\downarrow}{t} \\ & \times \sum_{n=1}^{\infty} \frac{1}{n^3} \sin^2\left(\frac{n\pi}{2}(1 + \frac{M}{M_S})\right) \\ & \cdot \frac{\sinh(n\pi \frac{t}{d_\uparrow + d_\downarrow}\sqrt{\frac{Q+1}{Q}})}{\sinh(n\pi \frac{t}{d_\uparrow + d_\downarrow}\sqrt{\frac{Q+1}{Q}}) + \sqrt{\frac{Q+1}{Q}}\cosh(n\pi \frac{t}{d_\uparrow + d_\downarrow}\sqrt{\frac{Q+1}{Q}})} \end{aligned} \tag{5}$$

Note that equation (5) is strictly valid and quantitative only when the domain wall width is far smaller than the film thickness t. For lower thickness an extended form can be used [18] that confirms the dominant role of the dipolar length and validates the use of equation (5) for qualitative discussion.
The equilibrium domain size is expressed by minimizing the total energy with respect to the domain period and the reduced magnetization, assuming the domain structure remains unchanged; the field behaviour is reflected by the hysteresis loops.

The basic equations derived from the competition between the different energy terms guide the understanding of nanostructure magnetism. They successfully describe the

behaviour of cobalt [16], FePd [13, 19] and FePt [20] films of different thicknesses and anisotropy constants.

3. Sample properties, preparation and experimental techniques

Previously, layers of chemically ordered FePd alloys *have been investigated* [19, 14, 13]. *They exhibited a strong perpendicular magnetocrystalline anisotropy with a ratio of the magnetic anisotropy to the magnetostatic energy well above 1.* Magnetic Force Microscopy images demonstrated *that the* magnetic configuration exhibited dramatic changes: *as the thickness of these FePd layer decreased from 30 to 5 nm, small (60 nm domain size) highly interconnected stripes were first observed, that turned into a complicated pattern mixing large stripes (600 nm) and sometimes bubbles (200 nm)* [19]. The corresponding hysteresis loops were elongated for large thickness with large saturation field whereas they exhibited a significant remnance and coercivity for thinner films. As the thickness of the layer increases, the domains' equilibrium size **decreases.** In 10 nm films of FePt with a saturation magnetization of 720 emu/ cm^3, a value of 5 $\times$ 10^6 erg/cm^3 for the anisotropy constant led to a calculated period of 50 nm in the demagnetized state whereas a value of about 10^7 erg/cm^3 led to a period of 200 nm [20]. Due to the reduced thickness and magnetization, the measured polar hysteresis loops of such films had an almost total remnance. In such FePt (FePd) films, chemical ordering tunes the anisotropy constant and hence, in principle, the subsequent domain pattern.

As shown by equation (5), increasing the anisotropy or thickness enhances the domain wall energy; hence, the smaller the number of domain walls, the larger the domains and the larger the demagnetizing factor. If the domain pattern is not conserved but converted into a large single domain, the demagnetizing factor $N_\perp$ is equal to 1 and films exhibit square and remnant hysteresis loops ($\frac{M}{M_S}$=1). *Since there is no wall anymore, the film energy is reduced to the Zeeman and the effective anisotropy energy,* as expressed by equation 6.

$$\begin{aligned} E = \quad & K_{eff} \sin^2\theta - M_S H \cos(\pi/2 - \theta - \alpha) \\ & \text{with } K_{eff} = K_u - 2\pi M_S^2 \end{aligned} \tag{6}$$

θ (respectively $\pi/2 - \alpha$) *is* the angle of the magnetization (respectively the field H) relative to the normal of the film and K_{eff} *is* the effective anisotropy constant, *that merges the magnetocrystalline anisotropy and demagnetizing energy.* Equation (6) relates the field to the magnetization orientation (as long the sample remains single domained) and is used for adjusting anisometry experiments [21].

Our samples were prepared by the technique described in references [22, 23, 13]. Molecular Beam Epitaxy (MBE) was performed on a 40 nm thick Pt(001) buffer layer epitaxially grown on a 2 nm seed layer of Cr deposited on MgO(001) substrate and annealed at $\sim 500^\circ$ to smooth the surface. FePt films of thicknesses of 2, 3, 5, 10 and 30 nm were prepared by alternate mono-atomic layer deposition at room temperature. The films were irradiated with 30 keV He^+ ions at fluences between 2×10^{13} and

1.2×10^{17} He^+/cm^2 at a temperature T=300°C. In order to avoid uncontrolled heating by the incoming beam, ion currents were kept below about 0.2 $\mu A/cm^2$. **In practice, irradiation was done in an additive way, each fluence being added to the previous one. In most cases, part of the sample was protected from additional irradiation so that a reference could be preserved.** The Standard MOKE in-field hysteresis loops were obtained using a λ= 633 nm laser, mostly with the magnetic field H applied perpendicular to the sample plane, i.e. in the polar geometry, PMOKE. The Polar Kerr Rotation (PKR) measured as a function of the applied field H was thus proportional to the magnetization out-of-plane component $M_\perp$. Magnetic anisotropy measurements were also performed: in samples with perpendicular anisotropy, the field was applied at a small angle from the film plane to drive a coherent rotation of the magnetization, monitored by PMOKE [21] and the effective anisotropy fields are deduced from the adjustment of the field-induced reversible part of the $M_\perp(H)$ curve. For films with an in-plane (and negative) anisotropy, the anisotropy field is simply determined from the onset of the saturation behaviour of $M_\perp(H)$ in an applied perpendicular field. **This is of course correct only if the loops are closed, and can lead to applied fields above 10 kOe, especially for the thinnest films.**

Magnetic domain patterns and remnant hysteresis loops were obtained from polar MOKE microscopy [4]. In this imaging technique, after saturating the sample, magnetic field pulses were applied to trigger the magnetization reversal but cancelled when collecting the MO signal on a CCD camera. Different states of the reversal process, frozen after switching the field off, were observed in this way. When the domain features were smaller than our resolution of about 400 nm, polar remnant (after zeroing the magnetic field) hysteresis loops were obtained from the magneto-optic intensity for different H values.

4. Experimental results

Firstly, a comparison of standard polar Kerr hysteresis loops obtained before (figure 1-a) and after (figure 1-b) irradiation at 300°C of as-grown FePt films by an ion fluence of 2×10^{14} He^+/cm^2 shows that the previously observed perpendicular anisotropy increase due to irradiation also holds for much thinner films [8]. For films of thickness 10 nm or below, they clearly provide a signature of the $L1_0$ phase transformation under irradiation. *The* fluence required to rotate the anisotropy is far lower in *these* thinner films than in the 40-50 nm films of reference [8]. These results are significant, *and* the hysteresis cycle shapes warrant detailed investigation, *reported below.*

The thinnest as-grown films exhibit an in-plane magnetic anisotropy, as evidenced by the slow field dependence of the $M_\perp(H)$ signal. *The loops saturate* above (respectively around) 10 kOe for t_{FePt} = 2 nm (respectively 3 nm). *The 5 nm pristine film has an intermediate behaviour.* The partly elongated *shape of its hysteresis loop s*hows that the sample is not homogeneously perpendicularly magnetized at H =0. No domains could be seen in this as-grown film by PMOKE microscopy, but a square remnant

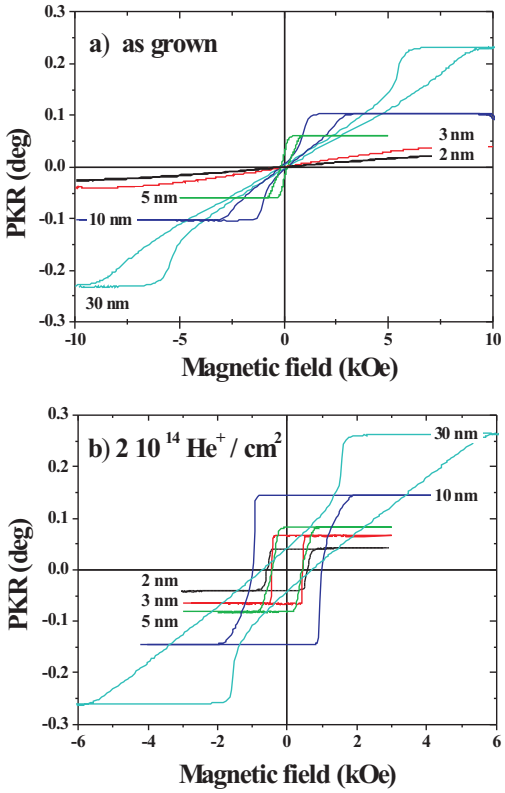

Figure 1. (Color online) PMOKE magnetic hysteresis loops of FePt films of increasing thickness, as noted in the figure a) As grown. b) After irradiation with 2×10^{14} He^{+}ions/cm^2 at 300°C.

hysteresis loop (not shown) was reconstructed from the PMOKE microscopy intensity, differing from the one obtained in field. This difference between remnant and in-field hysteresis loops can mean either that i) some regions of *this* sample (beyond our optical resolution) exhibit out-of-plane and remnant magnetization whereas others are perpendicular without remnance, or ii) *this* sample is single domain with tilted magnetization, combining two components : reversible tilted, and remnant out-of-plane. Thicker films (t=10 to 30 nm) exhibit hysteresis loops characteristics of out-of plane magnetic anisotropy but with a domain pattern consisting in stripes at zero field [17], in agreement with [16] and [19]. The PKR increases as the film thickness and saturates in the thickest films.

After irradiation, for all thicknesses, a most striking feature –besides the anisotropy evolution– is the reduction between the difference in coercive and of reversal field. For t=30 nm, the reversal field drops from 5.8 kOe after growth to 1.7 kOe after irradiation with 2×10^{14} He^{+} ions/cm^2; the coercive field increases to about 600 Oe under ion irradiation but the remnant magnetization is still at about 20% of the saturation value. In thinner films, the nucleation field decreases further and even equals the coercive field

for the thinnest films. The latter(t= 2, 3, 5, 10 nm) exhibit then a square and fully remnant polar loop. The coercive fields are weak, around 500 Oe for t=2-5 nm and about 1 kOe for t=10 nm **whereas it is about 3 or 4 times larger in thermally ordered samples of the same thickness [20]**. In addition, the PMOKE value at saturation increases rapidly (a factor of 80% between D=0 and 2×10^{14} He^+ ions/cm^2) and saturates progressively for higher fluences. This huge MO effect is known as a signature of partial chemical ordering, obtained here by ion irradiation [12].

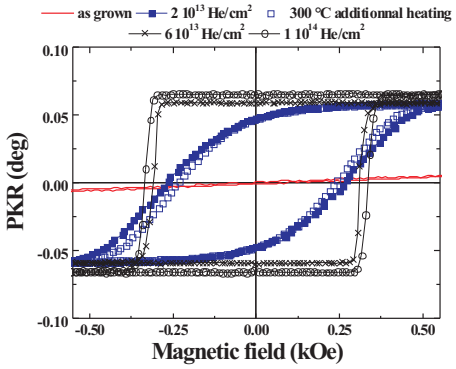

Figure 2. (Color online) PMOKE magnetic hysteresis loops of a t_{FePt} =3 nm film after irradiation with increasing fluences up to 10^{14} He^+ions/cm^2 at 300°C. For comparison, the hysteresis obtained on a part of the sample protected from the irradiation stage between 2 to 6×10^{13} ions/cm^2 but heated at 300°C is reported.

An investigation of the irradiation-induced MA transition from in-plane to out-of-plane was performed on the thinnest films. Figure 2 shows in-field polar hysteresis loops of the t_{FePt} =3 nm film for fluences increasing from 2×10^{13} up to 10^{14} He^+ions/cm^2. The initially in-plane magnetic anisotropy is drastically modified by an irradiation fluence as low as 2×10^{13} He^+ions/cm^2, which leads to an open out-of-plane polar hysteresis. During the next irradiation stage, part of the film was heated to the same temperature (300°C) but protected from ion irradiation in order to monitor any influence of the heating alone on the magnetic properties. The hysteresis loop of the latter area was indeed identical to that of the sample irradiated with a fluence of 2×10^{13} He^+ions/cm^2 (empty and full squares, figure 2) whereas the further irradiated area (6×10^{13} He^+ions/cm^2) exhibited a fully remnant hysteresis loop. This confirms the possibility of improving the chemical order using very low fluence heating at moderate temperature, whereas heating alone is unefficient.

However, the in-plane to out-of-plane transition is affected by the initial film growth features. This is evidenced by a detailed study performed on a t_{FePt}=5 nm film (figure 3-a). The in-field polar loop was square after irradiation to again only 2×10^{13} He^+ions/cm^2 at 300°C, indicating a single domain structure and remnant state of the magnetization, whereas its as-grown counterpart showed barely no remnance (figure 1-a). A series of PMOKE microscopy images is shown in figure 3-b. Analysis of the domain structure

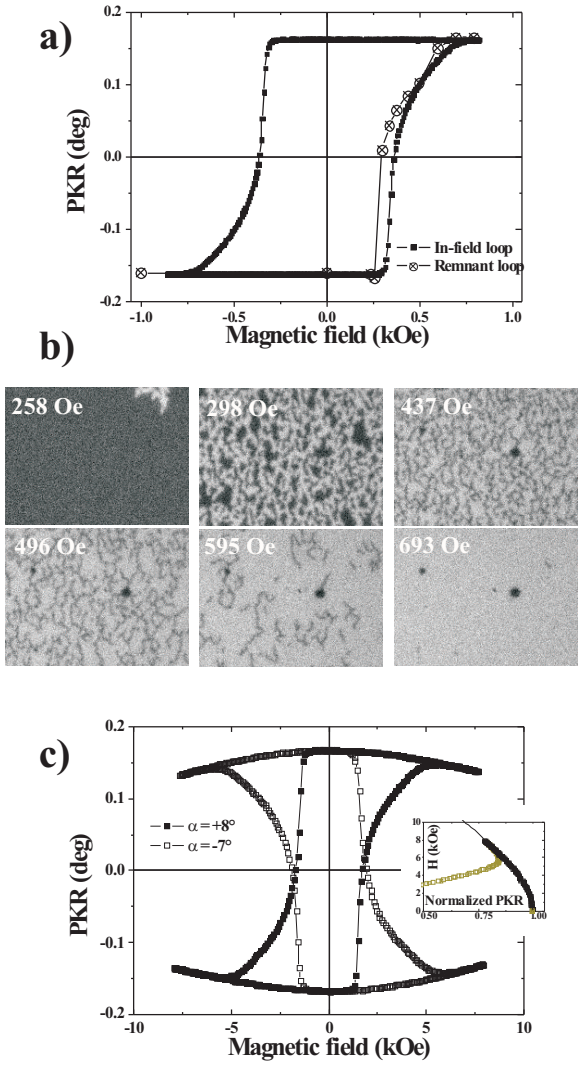

Figure 3. (Color online) For a $t_{\mathrm{FePt}} = 5$ nm film after irradiation with 2 10^{13} He^{+}ions/cm^2 at 300°C: a) MOKE hysteresis loops obtained during the magnetic field's sweeping – 25 s per loops – (full squares) and in the remnant state (crosses); the latter is obtained from the relative evolution of the intensity in PMOKE microscopy, as detailed in the text and was normalized to PKR loop. b) PMOKE images (10 μm x 13.5 μm) of the magnetic configuration when describing the hysteresis loop. c) PMOKE curves for 2 opposite angles of the applied field with respect to the sample plane used to deduce the anisotropy fields from the reversible parts of the loops, as shown in the insert.

at the early nucleation stage ($H = 258$ Oe) shows the presence of stripes**, entering the field of view in the top right corner,** of about 0.7μm in width. A further field increase ($H = 298$ Oe) induces a significant reversal with a ramified structure. Dendritic patterns develop and domain wall propagation is apparently controlled by structural disorder or inhomogeneities, as well as by demagnetizing effects. Full saturation is finally obtained at a much larger field ($H = 700$ Oe). The remnant hysteresis loop constructed

from the PMOKE images intensity is now practically identical to the one recorded during field sweeping (figure 3-a). To determine the effective magnetic anisotropy, anisometry experiments were performed and typical results are shown in figure 3-c for 2 values of the angle α between the sample plane and the external magnetic field. Adjusting the reversible part of the experimental $H = f(\theta)$ curve provides access via equation (6) to the anisotropy constant [21]. For our 5 nm thick FePt film irradiated with 2×10^{13} He^+ions/cm^2, an anisotropy field of about 10000 Oe is determined. The bulk saturation magnetization is 1100 emu/cm^3 [10]; however, in FePt films, a large spread is observed in the data [20, 24, 25], ranging from 400 to 1100 emu/cm^3. Assuming a middle range value of M_S, we obtain an anisotropy constant K_u of a few 10^6 erg/cm^3 for this film, smaller than the bulk anisotropy constant of ordered alloys (about 10^8 erg/cm^3 [10]) but leading to a quality factor above 1. Moreover, this 5 nm thick film combines a relatively small coercive field with a large anisotropy.

Finally, the effect of large irradiation fluence was also tested. For all film thickness, there was a threshold fluence above which the initial increase in out-of-plane anisotropy is partly lost again. This threshold increases as thicker layers are involved. **It was found to be around 3×10^{15} He^+ions/cm^2 for 2 nm thick films. For a t=10 nm FePt film (figure 4) and at the same dose, the loop is still remnant (similar to the 1.2×10^{15} He^+ions/cm^2 one) whereas the threshold has been passed for 2×10^{16} He^+ions/cm^2**. Above the threshold, hysteresis loops change from square and remanent to more rounded. By further increasing the field, the magnetization falls in the sample's plane.For FePt films as thick as 30 nm, the irradiation leads to a significant reduction of the nucleation field (See figure 1) but a complete remnance was not obtained. *For this thick 30 nm film, it was possible to use X-ray diffraction (XRD) using Cu-Kα radiation to investigate the structure with a reasonable signal to noise ratio, never achievable for thinner films.* The existence of $L1_0$ phase was evidenced by the appearance of additional (001) diffraction peaks for fluences above 10^{15} He^+ions/cm^2. This is in agreement with our previous results on FePd and FePt [8]. Again, increasing the fluence above 10^{16} He^+ions/cm^2 led to a deterioration of chemical order, a drop in the (001) peak intensity and ultimately to in-plane magnetization.

5. Discussion

Irradiation at temperatures where vacancies are sufficiently mobile allows successive pairwise exchange of atoms, as previously [8] described. The process relies on low-energy light ion irradiation in order to control small energy transfers and minimize recoil displacements. For instance, in a 2 nm thick FePt film, a 30 keV ion produces on average about 0.4 vacancies per incoming ion and, due to thermal and athermal recombinations, far less than 10% of these are actually effective in producing pairwise exchanges. This process is, in our view, the sole driving force for $L1_0$ phase formation at 300°C. Moreover, the vacancy lifetime is limited by capture at the surface, interfaces or defects : a simple estimate of the capture probability in our experimental conditions

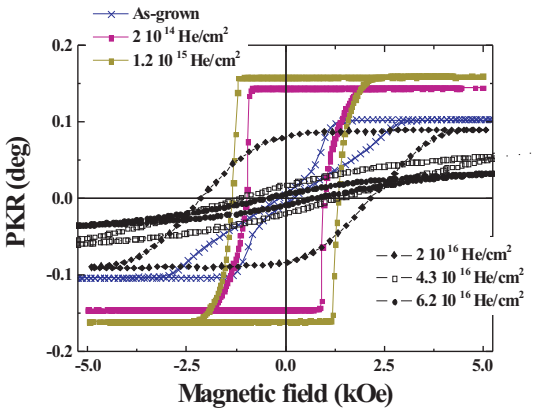

Figure 4. (Color online) MOKE hysteresis loops **in** a $t_{\mathrm{FePt}} = 10$ nm film after irradiation with increasing fluences of 30 keV He ions at 300°C

shows that there is very rarely more than a single vacancy at a time in the film. The influence of interfaces is obvious for the thinnest films but our results show also that the magnetization changes in successively thinner films are not limited to the effects of irradiation alone. The structural evolution under growth of pristine films, as remarkably illustrated in reference [13, 14] was shown by those authors to determine the magnetic properties. It certainly also affects vacancy capture as well as the direction and range of the local $L1_0$ ordering process. The dentritic domain structures (figure 3b) testifies to this, and suggests that more detailed combined studies, via microscopic probes, have to be performed in order to determine how this rather special irradiation-induced phase transformation occurs (via small $L1_0$ cluster formation, percolation and thermal relaxation...) and how this builds up the magnetocrystalline anisotropy in the films. The results certainly demonstrate the extreme sensitivity of the magnetic anisotropy to local order and short-range structural changes. The obtention of a perpendicular MA with perfectly square hysteresis cycles at very low fluences is quite remarkable in this respect. The effect is certainly enhanced by dealing with thinner films, for which the interface anisotropy easily overwhelms the magnetostatic anisotropy.

Note that in addition to the main process discussed above, there is also a small probability for permanent defect (dislocations, Fe or Pt clusters) buildup by vacancy trapping at existing growth-induced steps and dislocations. Such defects may accumulate over long irradiation fluences, randomizing the elemental repartition in the $L1_0$ zones, and leading the magnetization to flip back in-plane as observed at high fluences, above the 10^{16} He^{+}ions/cm^2 range. Extreme examples of this process are found in heavy ion beam irradiations such as those of 30 keV Ga focused ion beams (FIB) on, e.g., Pt/Co/Pt multilayers [26]. For the same initial 30 keV energy, the deposited collisional energy is about 100 times higher than for He, leading to displacement cascades,

and correspondingly to stable defects (and so-called "ion beam mixing" at the layer interfaces) that drastically modify the samples, even at relatively low fluences.

6. Conclusion

We have shown the effect of light (He^+) ion irradiation at low energy (30 keV) on FePt thin films as a function of film thickness. For the thinnest films, very low ion irradiation fluences induce a perpendicular magnetic anisotropy with very square hysteresis loops and small coercive fields. The reduced magnetostatic contribution in ultrathin films is an advantage. Obtaining such results at very low fluences is of obvious interest to lower the energy budget in applications. Of course, the potential advantages of these features may be limited or lost in applications requiring massive size reduction (e.g., ultrahigh density magnetic media) due to the micrometric size of the domains involved in the magnetic reversal, stemming from initial-stage film growth mechanisms. From a more basic viewpoint, our results suggest that a novel phase transformation process may be at work under irradiation.

Acknowledgments

Acknowledgments The authors wish to thank J. Moyaert and O. Kaitasov for technical assistance with the accelerator IRMA. This work was supported by the french ANR P-NANO under program CAMAIEU.

References

[1] J. Fassbender and J. McCord. Magnetic patterning by means of ion irradiation and implantation. *J. Magn. Magn. Mat.*, 320:579, 2008.

[2] T. Devolder and H. Bernas. Magnetic properties and ion beams: why and how. *Topics Appl. Physics*, 116:227–254, 2010.

[3] J. Fassbender, D. Ravelosona, and Y. Samson. Tailoring magnetism by light ion irradiation. *J. Phys. D: J. Appl. Phys*, 37:R179, 2004.

[4] J. Ferré and J.-P. Jamet. volume 3, page 1710. J. Wiley & sons, 2007.

[5] C. Chappert, H. Bernas, J. Ferré, V. Kottler, J.-P. Jamet, Y. Chen, E. Cambril, T. Devolder, F. Rousseaux, V. Mathet, and H. Launois. Planar Patterned Magnetic Media Obtained by Ion Irradiation. *Science*, 280:1919–1922, 1998.

[6] T. Devolder, S. Pizzini, J. Vogel, H. Bernas, C. Chappert, V. Mathet, and M. Borowski. X-ray absorption analysis of sputter-grown Co/Pt stackings before and after helium irradiation. *Eur. Phys. J. B*, 22:193, 2001.

[7] T. Devolder, H. Bernas, D. Ravelosona, C. Chappert, S. Pizzini, J. Vogel, J. Ferré, J.-P. Jamet, Y. Chen, and V. Math. Ion beam induced magnetic nanostructure patterning. *Nucl. Inst. and Meth. B*, 175:375–381, 2001.

[8] H. Bernas, J.-Ph. Attané, K.-H. Heinig, D. Halley, D. Ravelosona, A. Marty, P. Auric, C. Chappert, and Y. Samson. Ordering intermetallic alloys by ion irradiation: A way to tailor magnetic media. *Phys. Rev. Lett.*, 91:077203, 2003.

[9] D. Ravelosona, C. Chappert, V. Mathet, and H. Bernas. Chemical order induced by ion irradiation in FePt (001) films. *Appl. Phys. Lett.*, 76:236, 2000.

[10] R. F. C. Farrow, D. Weller, R. F. Marks, M. F. Toney, S. Hom, G. R. Harp, and A. Cebollada. Growth temperature dependence of long-range alloy order and magnetic properties of epitaxial FePt films. *Appl. Phys. Lett.*, 69:1166, 1996.

[11] R. F. C. Farrow, D. Weller, R. F. Marks, M. F. Toney, A. Cebollada, and G. R. Harp. Control of the axis of chemical ordering and magnetic anisotropy in epitaxial FePt films. *J. Appl. Phys.*, 79:5967, 1996.

[12] A. Cebollada, D. Weller, J. Sticht, G. R. Harp, R. F. C. Farrow, R. Marks, R. Savoy, and J. C. Scott. Enhanced magneto-optical Kerr effect in spontaneously ordered FePt alloys: Quantitative agreement between theory and experiment. *Phys. Rev. B*, 50:3419, 1994.

[13] D. Halley, Y. Samson, A. Marty, P. Bayle-Guillemaud, C. Beign, B. Gilles, and J. E. Mazille. Anomaly of strain relaxation in thin ordered fepd layers. *Phys. Rev. B*, 65:205408, 2002.

[14] David Halley. *Croissance, mise en ordre chimique et relaxation des contraintes épitaxiales dans des alliages FePd et FePt.* PhD thesis, University Joseph Fourier, Grenoble, 2001.

[15] C. Kittel. Theory of the structure of ferromagnetic domains in films and small particles. *Phys. Rev.*, 70:965, 1946.

[16] M. Hehn, S. Padovani, K. Ounadjela, and J. P. Bucher. Nanoscale magnetic domain structures in epitaxial cobalt films. *Phys. Rev. B*, 54(5):3428–3433, 1996.

[17] C. Kooy and U. Enz. *Philipps Res. Rep*, 15:7, 1960.

[18] V. Gehanno, Y. Samson, A. Marty, B. Gilles, and A. Chamberod. Magnetic susceptibilities and magnetic domain configuration as a function of the layer thickness in epitaxial fepd(001) thin films ordered in the $l1_0$ structure. *J. Magn. Magn. Mat.*, 172:26–40, 1997.

[19] V. Gehanno, A. Marty, B. Gilles, and Y. Samson. Magnetic domains in epitaxial ordered FePd(001) thin films with perpendicular magnetic anisotropy. *Phys. Rev. B*, 55:12552, 1997.

[20] F. Casoli, L. Nasi, F. Albertini, S. Fabbrici, C. Bocchi, F. Germini, P. Luches, A. Rota, and S. Valeri. Morphology evolution and magnetic properties improvement in FePt epitaxial films by in situ annealing after growth. *J. Appl. Phys.*, 103:043912, 2008.

[21] V. Grollier, J. Ferré, A. Maziewski, E. Stefanowicz, and D. Renard. Magneto-optical anisometry of ultrathin cobalt films. *J. Appl. Phys.*, 73:5939, 1993.

[22] V. Gehanno, C. Revenant-Brizard, A. Marty, and B. Gilles. Studies of epitaxial Fe0.5Pd0.5 thin films by x-ray diffraction and polarized fluorescence absorption spectroscopy. *J. Appl. Phys.*, 84:2316, 1998.

[23] D. Halley, Y. Samson, A. Marty, C. Beigné, and B. Gilles. Surface morphology and chemical ordering in FePd/Pd(0 0 1) thin layers. *Surface Science*, 481:25, 2001.

[24] J. Yu, U. Ruediger, A. Kent, R.F.C Farrow, R.F. Marks, D. Weller, L. Folks, and S.S. Parkin. Magnetotransport and magnetic properties of molecular beam epitaxy L10 FePt films. *J. Appl. Phys.*, 87:6854, 2000.

[25] K. Barmak, J. Kim, L. H. Lewis, K. R. Coffey, M. F. Toney, J. Kellock, and J.-U. Thiele. On the relationship of magnetocrystalline anisotropy and stoichiometry in epitaxial L10 CoPt (001) and FePt (001) thin films. *J. Appl. Phys.*, 98:033904, 2005.

[26] J. Jaworowicz, A. Maziewski, P. Mazalski, M. Kisielewski, I. Sveklo, M. Tekeliak, V. Zablotskii, J. Ferré, N. Vernier, A. Mougin, A. Henschke, and J. Fassbender. Spin reorientation transitions in Pt/Co/Pt films under low dose Ga+ ion irradiation. *Appl. Phys. Lett.*, 95:22502, 2009.